P-ISSN 2586-9000
E-ISSN 2586-9027
Homepage : https://tci-thaijo.org/index.php/SciTechAsia
Science & Technology Asia
Vol.28 No.2 April - June 2023
Page: [112-124]
Original research article

Design and Analysis of the Ladder Impact Attenuator Structure According to EN1789:2020 using Explicit Dynamics

Khemapat Tontiwattanakul[1], Phadungsak Rattanadecho[2], Chartchay Chumchan[3,*]

[1]*Department of Mechanical and Aero-space Engineering, Faculty of Engineering, King Mongkut's University of Technology North Bangkok, Bangkok 10800, Thailand*
[2]*Department of Mechanical Engineering, Faculty of Engineering, Thammasat University, Pathum Thani 12120, Thailand*
[3]*Department of Power Engineering Technology, College of Industrial Technology, King Mongkut's University of Technology North Bangkok, Bangkok 10800, Thailand*

Received 31 August 2022; Received in revised form 7 September 2022
Accepted 18 September 2022; Available online 14 June 2023

ABSTRACT

This paper presents a design of cost-effectiveness and testing equipment for a ladder impact attenuator. The design goal is to create the attenuator structure as a multi-step in crash testing facility such that acceleration pulse profile is generated in accordance with EN1789, which is an international standard for assessing crashworthiness and crash compatibility for ambulances. The preliminary design of the impact attenuator structure is that some appropriate values of spring stiffness of the impact attenuator were estimated analytically. The impact attenuator structure is placed in a transverse direction as a ladder and has a multi-layered tubular shape to obstruct and absorb impact energy. Explicit dynamics finite element method was used to verify and validate with experimental data, that the crash results are permanent flexural large deformations. The simulation result was validated by experimental data of acceleration pulse profile, it is found that good tendency. The experiments have shown that the structure of the ladder impact attenuator can stop the sled movement within the desired time and displacement.

Keywords: Ambulance crashworthiness; Explicit dynamics; EN1789:2020; Impact Attenuator

1. Introduction

Currently, emergency health services are available by land, sea, and airway. Ambulances play an important role in emergency health services. Since the demand for road ambulances has increased, accidents in the case of road ambulances are also increased. Some major causes of accidents are driving speed and quick transportation.

***Corresponding author:** chartchay.c@cit.kmutnb.ac.th **doi:** 10.14456/scitechasia.2023.31

Medical personnel and patients are at high risks in terms of serious injury or death in the accidents. The National Highway Traffic Safety Administration (NHTSA) provided information on ambulance accidents from 1992 to 2011 showing that 17% of drivers and 29% of passengers were injured. In contrast, 4% of drivers and 29% of ambulance passengers die in ambulance-related accidents in the United States, with further research and development on ambulances and ambulance equipment [1]. In Thailand, the National Institute for Emergency Medicine, the Ministry of Public Health of Thailand, is aware of the safety of ambulance use and has issued requirements for ambulance manufacturers to use EN1789:2020 [2], which is a standard in crashworthiness and crash compatibility for ambulance production. EN1789 specifies some requirements to manufacturers regarding guidelines for design, safety, testing and performance of road ambulance transportation.

The standard proposes an assessment of the crashworthiness of the ambulance cabin and medical device attachment by assessing the damage in 5 directions $(\pm x, \pm y, +z)$ both in the case of static tests and dynamic crash tests. For the dynamic crash tests, i.e., in the longitudinal (front crash), transverse (side crash), and vertical (roof crash) directions, the ambulance cabin and medical devices in the test are required to be mounted on a sled. The main purpose of this test is cost-effectiveness and collision damage investigation of ambulance cabins and medical equipment. An ambulance cabin and medical equipment in the test will speed up to 30-32 km/h and crash with an impact attenuator aiming to generate an acceleration pulse profile in accordance with one specified in EN1789.

This work proposes the design and construction of a low-cost crash testing facility for ambulances with a maximum 1,400 kg of cabin mass. It is very important that the collision acceleration pulse profile comply with the one specified in EN1789:2020. This research also presents the design procedure of an impact attenuator (IA) to absorb collision energy and maintain a consistent acceleration pulse profile.

Based on the reviews of previous research to get the conceptual design, preliminary shape, and investigation method, it was found that impact attenuation structures used in automobiles. In order to gain better understanding of the process of absorbing energy, many studies have analyzed the behavior of typical tubular structures under axial impact conditions [3, 4]. The most common element is called a "crash box" which is connected between the automobile cabin and front bumper structure and mostly made of steel [5, 8, 9] and aluminum [9-11]. Satosa et al. [12] applied the honeycomb material to the design of the bumper structure of automobiles, which is lightweight and has good collision energy dissipation capability. Ghasemnejad et al. [13] proposed the design of corrugated crash boxes for automobile bumpers to achieve the lowest crush force fluctuation capability; the energy absorption and axial crushing during crash velocity at 25 m/s were predicted by using an explicit dynamics finite element model. Yang et al. [14] presented the comparison results of greatly enhanced energy absorption of a multi-cell hexagonal tube versus a single tube under crushing axial force of crash at 10 m/s in which the results were represented by using experiments and explicit dynamics finite element analysis. Segade et al. [15] developed a lightweight crash box for a student formula car with pyramid shape, which was welded from an aluminum alloy sheet.

The research above suggests the impact attenuator for crash energy absorption structure for automobiles, but the shape is quite complex and has high production costs. Moreover, considering crash results exposed in past research [15-18], it was found that the acceleration magnitude was higher than the author's desire because the crash box geometries have a very high degree of stiffness.

This research presents the design and analysis of an impact attenuator structure as explicit dynamics finite element method for

low-cost crash testing facility to generate the acceleration pulse profile in accordance with EN1789:2020.

2. Preliminary Design of Impact Attenuator

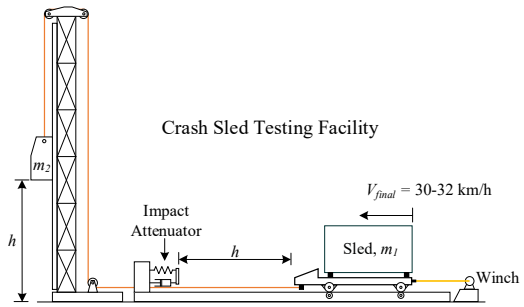

Fig. 1. Diagram of conceptual design of the low-cost crash testing facility.

Fig. 1 shows the conceptual design diagram of the crash testing facility. The ambulance cabin or/and medical devices can be installed on the sled (m_1 = 1,400 kg) and the front end of the sled is connected to the drop mass (m_2 = 3,200 kg) hanging from a pulley on a truss tower by using wire rope. The drop mass is raised and suspended to be height (h) by pulling with an electric winch between the rear of the sled and the end of the rail. The final velocity before crash can be determined by calculating the height of the drop mass as Eq. (1). The crash testing can be started by disconnecting the sled from the winch. The sled is then accelerated to the desired velocity (30-32 km/h) and the front end of the sled collides with the impact attenuator. The acceleration pulse profile is measured by using an accelerometer mounted on the ambulance cabin, medical device, and sled frame.

$$V_{final} = \sqrt{\frac{2gh\left(m_2 - \mu m_1\right)}{m_1 + m_2}}, \qquad (2.1)$$

where V_{final} is final velocity of the sled before crash (m/s), g is gravitational constant (m/s^2), h is the height of the drop mass (m), μ is friction between sled wheel and rail road, m_1 is sled mass (kg), and m_2 is drop mass (kg).

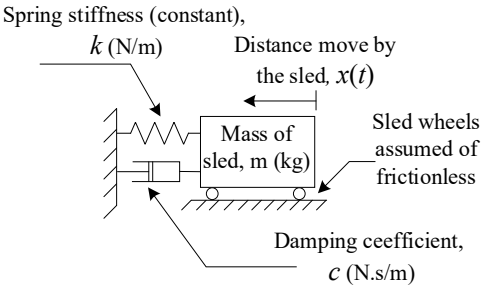

Fig. 2. Lumped mass system model.

The impact attenuator is a barrier in the low-cost crash testing facility to decelerate and stop the sled, which itself is permanently deformed. To prevent acceleration pulse profile overshoot out of the standard, the appropriate stiffness of the impact attenuator was initially determined by using Hooke's Law. In the preliminary study, impact attenuator stiffness was assumed to be a linear spring such that the acceleration or deceleration, velocity and displacement form crash were predicted by using the collision model as lumped mass system model with single degree of freedom (DOF) [19, 20], seen in Fig. 2.

$$m\frac{d^2x(t)}{dt^2} + c\frac{dx(t)}{dt} + kx = x(t), \qquad (2.2)$$

where m is the mass of sled (kg), c is the damping coefficient (N.s/m), k is the spring constant (N/m) and x is the displacement (m).

This section shows analytical calculations to estimate spring constant value. The maximum acceleration was determined during the impact ($a_{\max}$) as about 10g and the sled mass as 1,400 kg. It may be calculated average of crushing force (F_{ave}) as follows:

$$\begin{aligned} F_{avg} &= ma_{\max} \\ &= 1{,}400\,\text{kg} \times 10g \times 9.81\,\text{m/s}^2 \\ &= 137{,}340\,\text{N}. \end{aligned} \qquad (2.3)$$

In this paper, the spring was maximally compressed at 0.5 m. Therefore, the spring constant (k) was

$$k = \frac{F_{avg}}{\delta} = \frac{137{,}340\,\text{N}}{0.5\,\text{m}} = 274{,}680\,\text{N/m}, \quad (2.4)$$

and the damping factor can be calculated by

$$c = 2\zeta\sqrt{k.m}. \quad (2.5)$$

From Eq. (2.2), the collision model was modelled by using MATLAB/ Simulink (see Fig. 3.) with initial velocity as 8.5 m/s to predict the transient response of crash, i.e., displacement, velocity and acceleration as well as the end time of the collision. According to Eq. (2.5), the damping ratio (ζ) of the impact attenuator structure was difficult estimation. In the case of the lumped mass system model with 1 DOF can be defined as an undamped system, which transient response magnitude of mass was oscillated by perfectly elastic. The maximum acceleration at 100 m/s^2 and the collision deceleration time of approximately 0.15s were parameters used to determine the preliminary spring constant. The parametric study of the spring constant modified by differencing ±5% as three cases: k_1 = 288,414 N/m, k_2 = 274,680 N/m, and k_3 = 260,946 N/m. Moreover, an additional three cases with damped system were k_3+Damped.1, k_3+Damped.5, and k_3+Damped.1, in which three damping factors were calculated by using spring constant of k_3 with 3 damping ratios as 0.1 (3,827.7 N.s/m), 0.5 (19,113 N.s/m), and 1 (38,277 N.s/m), respectively.

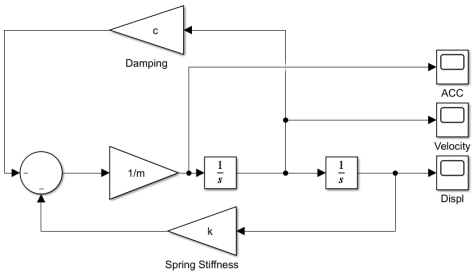

Fig. 3. The collision model of MATLAB /Simulink.

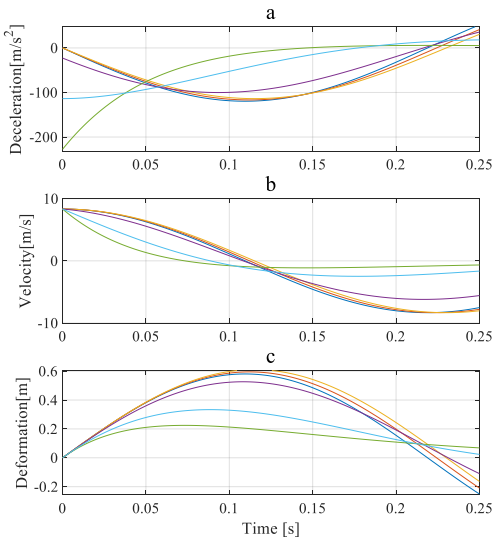

Fig. 4. Comparison of transient response results from parametric studies (see legend: — k_1, — k_2, — k_3, — k_3 with damping ratio 0.1, — k_3 with damping ratio 0.5, and — k_3 with damping ratio 0.5).

The simulation results of collision models of six parametric studies showed deceleration, velocity, and displacement as seen in Fig. 4. The results of the first 4 cases in Fig. 4a were collision models without damped and lower damped which is elastic collision. Only analyzing the first pulse, there are two collision stages. In the first stage, the spring of the impact attenuator was compressed until mass of sled momentarily stopped. In the second stage, the deformation stage and part of deformation were recovered and remained until the acceleration became zero which happened after the time at 0.218 s, 0.224 s, 0.230 s, and 0.231 s, respectively. In Fig. 4b, the sled velocity of each case was zero after

collision time at 0.109 s, 0.112 s, 0.115 s, and 0.108 s, respectively.

The simulation results of the three first cases showed sled velocity of zero at 0.115s with a maximum acceleration of 113.770 m/s^2 and displacement of 0.610 m (see Fig. 4c). It is found that the velocity of the sled becomes zero at 0.094 seconds after a maximum acceleration of 100.1323 m/s^2, and a smaller displacement of about 0.5265 m. A higher damping factor was able to significantly reduce the response magnitude of system as case 5 and critical damping of case 6. However, the spring constant with 260,946 N/m was chosen to design the geometry of the real impact attenuation structure.

3. Geometrical Design

The spring stiffness (k) of an impact attenuator structure is a value that indicates the ability to return the original shape when the load is removed. However, there is a condition that the force acting on the structure must not exceed the yield point, known as non-permanent deformation of the material. The impact attenuator structures were designed in some specific shapes with low stiffness in order to absorb the crash energy caused by large deformation. In this paper, the carbon steel tube was chosen to design the impact attenuator structure. Considering the length and cross- section to calculate stiffness of a tube, the axial crushing made higher axial stiffness than bending stiffness when compared with transverse direction to crash the cross member. Therefore, the bending stiffness was used and expressed in the Eq. (3.1) as follows:

$$k_{bending} = \frac{3EI}{L^3}, \qquad (3.1)$$

where $k_{bending}$ is bending stiffness (N/m), E is elastic modulas (GPa), I is area moment of inertia of cross section (m^4) and L is length (m). The area moment of inertia can be calculated as Eq. (3.2)

$$I = \frac{\pi\left(\frac{d_o^4 - d_i^4}{64}\right)}{12}, \qquad (3.2)$$

where d_o is outside diameter (m) and d_i is inside diameter (m).

From Eqs. (3.1) and (3.2), the bending stiffness of three diameters with same thickness of 0.0045 m of carbon steel tube was calculated as follows: the smallest hollow tube d_{o1} = 0.0605 m with long 1.7 m, the medium-sized hollow tube d_{o2} = 0.0763 m with long 1.7m, and the largest hollow tube, d_{o3} = 0.0889 m with long 1.5 m that all tubes were loosely stacked. The combination of three bending stiffnesses of the impact attenuator structure was 261,001.5 N/m as named item "IA1 or A-step" in Fig.5a that installation was done by inserting all tubes into the two supports through holes with radius of 0.45 m both left and right side, which are 1.7 m apart. In order to prevent the tubes slipping out of the supports after collision and large deformation, the smallest hollow tube and medium-sized hollow tube were extended to be 3 m by overhanging both sides of 0.65 m. However, the carbon steel tubes material is not spring steel; thus, bending stiffness of the impact attenuator structure is not constant over the entire deformation range. Therefore, to ensure that it can support the collision of a mass weighing 1,400 kg, it is steps ladder (addition B-step and C-step) and 0.2m apart. Fig. 5b shows "IA2" consists of 2 steps ladder with A-step and B-step. Fig. 5c shows "IA3" consists of A-step, B-step, and C-step, but C-step is only the medium-sized hollow tube. Fig.5d shows "IA4" consists of A-step, B-step, and C-step, but C-step is the smallest hollow tube and medium-sized hollow tube. Finally, Fig. 5e shows "IA5" consists of A-step, B-step, and C-step, but C-step is the smallest hollow tube, medium-sized hollow tube, and the largest hollow tube.

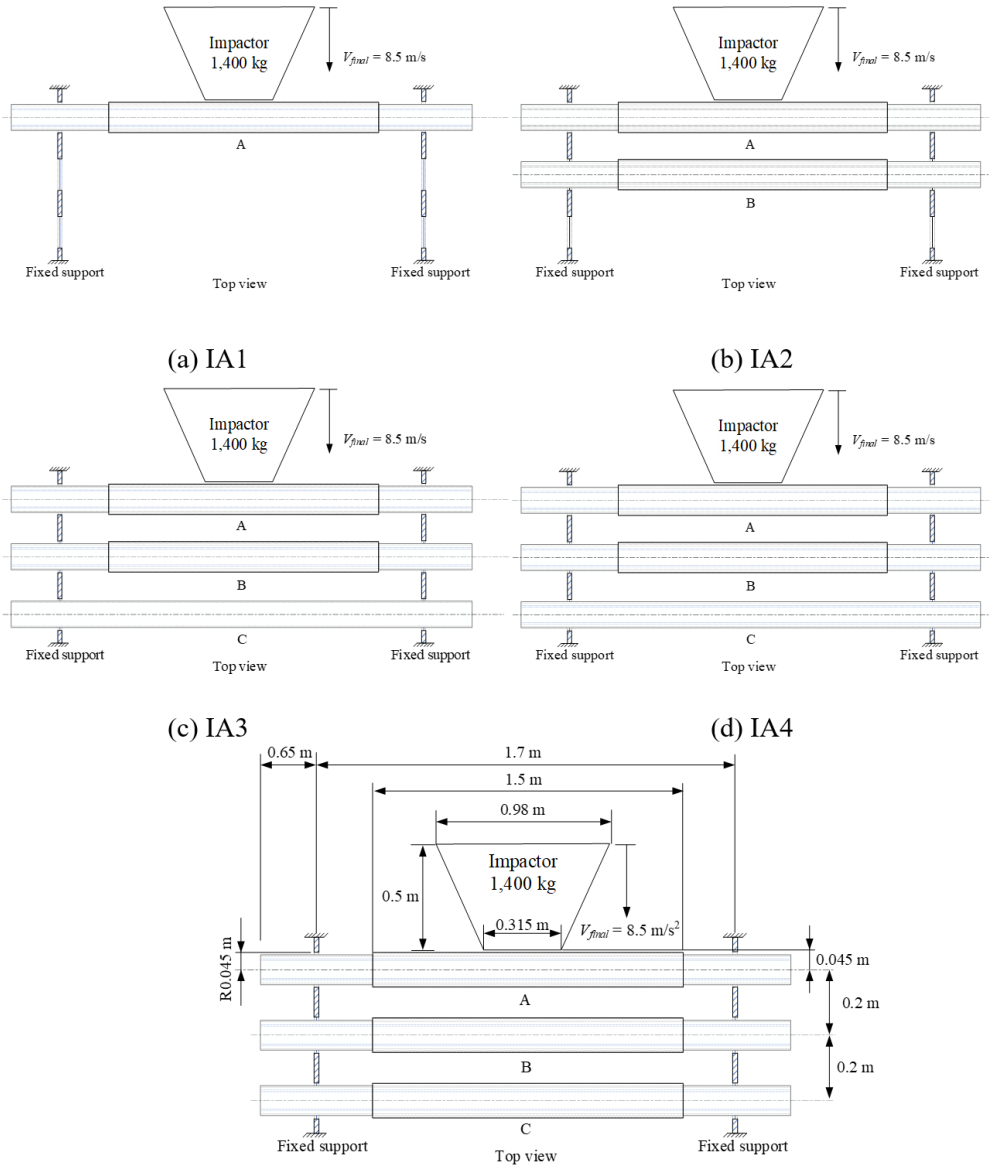

Fig.5. A diagram of the geometry and boundary conditions of 5 models of the ladder impact attenuators.

4. Governing Equations

A review of the relevant literature revealed that the ideal model was the explicit dynamics finite element model (FEM). This method is used to determine fundamental quantities such as velocity, displacement, and acceleration according to the initial conditions of displacement and velocity relative to time. The most important are composition stress, plastic stress, contract force, and energies such as kinetic energy, internal energy, contact energy and hourglass energy. The implicit methods are Beta Newmark integration scheme and Hilbert-Hughes Taylor software that uses these methods are: LS-DYNA-

Implicit, ABAQUS–Standard and Radioss-Implicit [21, 22].

A crash simulation is a virtual simulation of a destructive crash test of a vehicle and components using computer-aided analysis software. A computer-aided parametric design software is typically used for modeling automotive components, whose coordinates and geometric details are designed as CAD data; then the data can be transferred to FEM software. The finite element method consists of three main steps: (1) pre-processing is the step to create the finite element mesh to divide the geometry into subdomains, and determine the material properties and boundary conditions, (2) the solution procedure in FEM software processes solves the governing equations matrix for the primary quantities and (3) post-processing checks the validity of the solution, examines the values of primary quantities (such as displacements and stresses), and derives and examines additional quantities (such as specialized stresses and error indicators). The governing equations of transient dynamics [21, 23] are as follows:

$$[M]\left\{\frac{d^2u}{dt^2}\right\}+C\left\{\frac{du}{dt}\right\}+K\{U\}=\{F_{ext}(t)\}, \qquad (4.1)$$

where M = Mass matrix, C = Damping matrix, K = Stiffness matrix, F_{ext} = External force, t = Time.

In explicit time integration schemes the above equation can be written as:

$$[M]\left\{\frac{d^2u}{dt^2}\right\}_n+C\left\{\frac{du}{dt}\right\}_n+K\{U\}_n=\{F_{ext}(t)\}_n, \qquad (4.2)$$

where n represents a time snapshot of the pheominar. Physically, it refers to

Inertial force + Damping force +
Stiffness force = External force (4.3)

Using second order accurate explicit central difference operator $\left\{\frac{du}{dt}\right\}_n$ and $\left\{\frac{d^2u}{dt^2}\right\}_n$ can be expressed as

$$\left\{\frac{du}{dt}\right\}_n=\frac{\{U\}_{n+1}-\{U\}_{n-1}}{2\Delta t}, \qquad (4.4)$$

$$\left\{\frac{d^2u}{dt^2}\right\}_n=\frac{\{U\}_{n+1}-2\{U\}_n-\{U\}_{n-1}}{2\Delta t^2}, \qquad (4.5)$$

Substituting Eqs. (4.4) and (4.5) into Eq. (4.2), thus

$$\frac{1}{\Delta t^2}[M]+\frac{1}{2\Delta t}[C]\{U\}_{n+1}=\{F_{ext}\}_n-\{F_{\text{internal}}\}_n+\frac{1}{\Delta t^2}[M]\left[2\{U\}_n-\{U\}_{n-1}\right]+\frac{1}{2\Delta t}[C]\{U\}_{n+1}, \qquad (4.6)$$

where F_{internal} = Internal force

Eq. (4.6) is the main equation for explicit dynamic simulation.

5. Material Property

The finite element modeling for explicit dynamics analysis of non-linear materials used plastic and elastic properties, for which the tress-hardening and true stress-strain diagrams are required. The properties of mild steel, which is the material used for the impact attenuator, in ambient temperature are obtained by tensile testing [24].

This research uses a commercially available material called JIS-SS400 standard carbon steel with a density of 7,850 kg/m^3, modulus of elasticity 213,480 MPa, and Poisson's ratio 0.3. The true stress-strain relationship was non-linear data [25] as shown in Fig. 6.

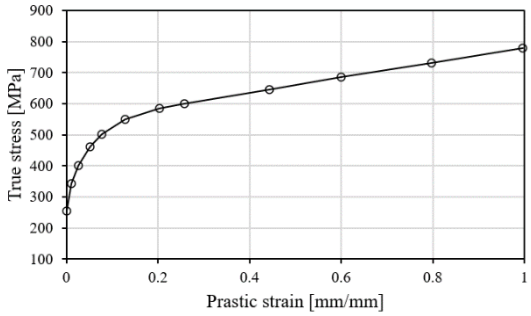

Fig. 6. The stress-strain relationship graph of JIS-SS400 material.

6. Finite Element Modeling

The CAD design of the ladder impact attenuator was shell geometries for ANSYS Mechanical (ANSYS Inc., Canonsburg, PA, USA). The Ansys Workbench/Ls-Dyna [23, 26] was used to define initial and boundary conditions, and for solving parameters, meshing, and posting results. In Fig. 7, the boundary condition details of surface body of frontal sled, called the "Impactor", specified stiffness behavior with rigid, 0.01 m of thickness and linear structure steel. The point mass option was used to apply mass of 1,400 kg at the centroid position of impactor. The rigid body constraint option is defined as freely moveable in only the *x*-direction and the initial condition is defined as a velocity of 8.5 m/s. The surface bodies of support are specified stiffness behavior with rigid, 0.01 m of thickness and linear structure steel, which boundary condition is fixed support (i.e. it cannot move or rotate in any direction). The connection model of all bodies is defined by using insert body interaction and define frictional with friction coefficient of 0.2.

The body contact tracker option was used to track the contact force at the frontal sled. The surface bodies of tubes of the ladder impact attenuator specified stiffness behavior with flexible, 0.0045 m of thickness and material property, which plasticity option and multi-nonlinear isotropic hardening were used to define the material from test data of stress-strain relationship in Fig. 6.

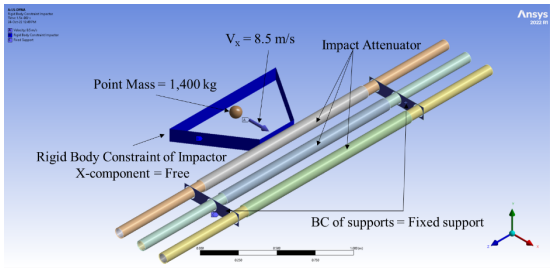

Fig. 7. The IA5 configuration of ladder impact attenuator structure in the ANSYS/Ls-Dyna program.

The time step value is a very important factor affecting the solution convergence to validate results and sufficient quality for an explicit dynamic study. Therefore, the minimum time step was determined by the well-known Courant-Friedrichs-Levy (CFL) condition with a safety factor of 0.9. The end time of the collision was used at 0.15 s and the number of calculating resolutions was set at 50 values.

The mesh quality is important to accurate simulation results. The mesh size is optimized by using the mesh independent method. FEM meshing was modeled by using shell element with 4-node linear elements, which model of IA1 was used to study the mesh independence and to balance the convergence results and computational time spent. The mesh independent studies were four resolutions: mesh model 1 with a mesh size of 0.03 m (5,167 elements), mesh model 2 with a mesh size of 0.02 m (9,205 elements), mesh model 3 with a mesh size of 0.01 m (20,290 elements) and a mesh model 4 with a mesh size of 0.008 m (31,903 elements). Fig. 8 shows that the mesh size 0.01m have similar results of stress and deformation with the mesh size of 0.008 m. The time savings is important for studies with more complex structures, so the following studies have used a mesh size of 0.01 m, which the number of meshes of IA1, IA2, IA3, IA4, and IA5 were 37,414, 44,614, 50,314, 50,314, and 54,514 elements, respectively.

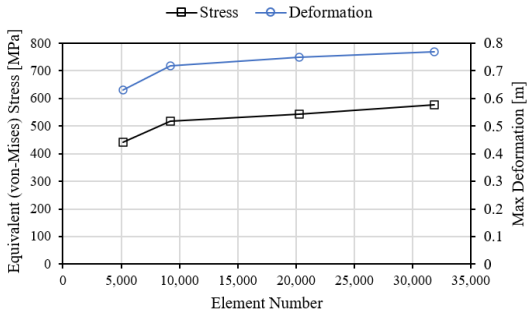

Fig. 8. Mesh independent analysis curves comparing stress and deformation of the IA1 model using mesh sizes ranging from 0.030, 0.015, 0.010, and 0.008 m, respectively.

7. Results and Discussion

The five different models of the ladder impact attenuator to virtual crash tests and to ensure which model patterns are available practical. The explicit dynamics finite element analysis was used to predict collision with sled mass of 1,400 kg at velocity of 8.5 m/s, which the acceleration pulse profile vs collision time of each model was comparted acceleration threshold according to the EN1789 standard. The main result of this research is shown in Fig. 9. The black line, blue line, green line, yellow line, and red line are for IA1 to IA5, respectively. In addition, the lower and upper acceleration limits according to the EN1789 standard are represented by the light brown solid line and dash line. It can be seen that the result of model IA1 was below the threshold acceleration and final collision time was greater than 0.15 s. The simulation results of IA2, IA3, and IA4 were acceptable acceleration pulse profiles. Finally, the simulation result shows that IA5 slightly fluctuated above the upper limit at 120 m/s^2, but the acceleration fluctuation stops within the EN1789 boundary.

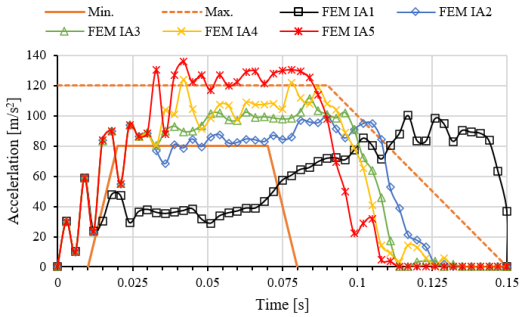

Fig. 9. The comparison results of the acceleration vs collision time with the EN1789 reference acceleration threshold.

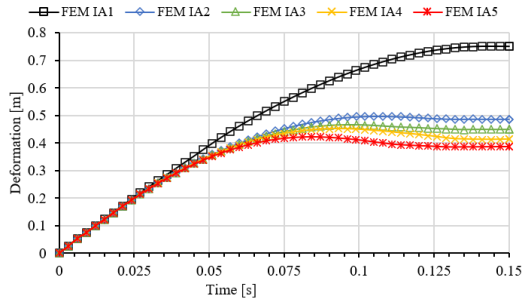

Fig. 10. Comparison results of displacement and collision time.

Additionally, Fig. 10 shows a comparison of the displacement of various IA models. It can be seen that the deformation IA1 case is higher than the design value at 0.5 m. This is consistent with the results of below the threshold acceleration. Fig. 11 compares different models during deformations at 0.05, 0.1 and 0.15s (see description in each picture). The simulation results of displacement analysis at the frontal sled shows that each model has the maximum displacement after the collision as follows: 0.7501 m for model IA1, 0.4974 m for model IA2, 0.46587 m for model IA3, 0.45157 m for model IA4, and 0.42274 m for model IA5.

Fig. 12 shows an isometric view of the results comparing stress distributions from the finite element analysis during a collision with a velocity of 8.5 m/s at 0.05, 0.1, and 0.15s (see description in each picture). It is found that the maximum stress of each model was 561.1 MPa, 550.9 MPa, 548.6 MPa, 546.3 MPa, and 547.2 MPa, respectively. It can be seen that the

IA1 model sustains the most damage, and the IA5 model sustains the least damage. It should be noted that the maximum stress of all cases is higher than the yield point of the material causing permanent deformation.

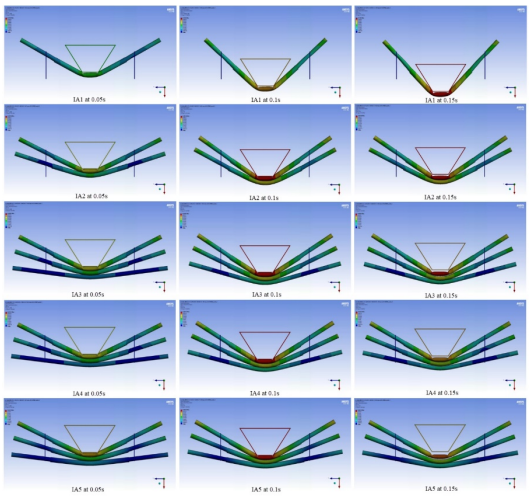

Fig. 11. Shows the simulation results comparing of the deformations at 0.05, 0.1 and 0.15 s.

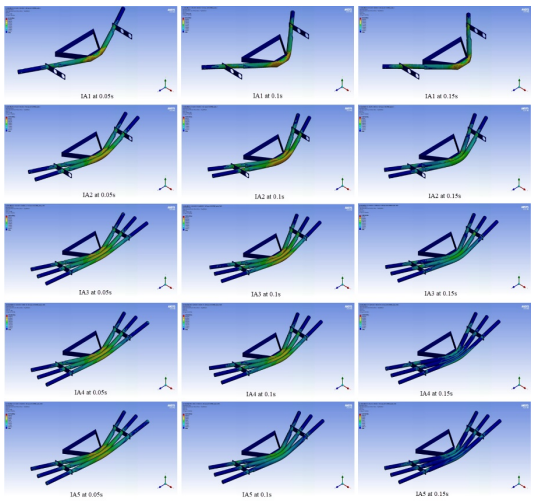

Fig.12. Shows the comparison results of stress distributions at 0.05, 0.1 and 0.15s.

8. Test and validation

The crash testing facility was equipped with accelerometer sensors at various points to verify the acceleration pulse profile according to EN1789 standard. The instruments consisted of a data acquisition system (Fig. 13(a)) (NI DAQ) which has 4 input channels (Fig. 13(b)) to connect 4 accelerometers type 4507B of Brüel & Kjær (Fig. 13(c)). The accelerometers were mounted on the sled to measure in the crash direction (Fig. 13(d)).

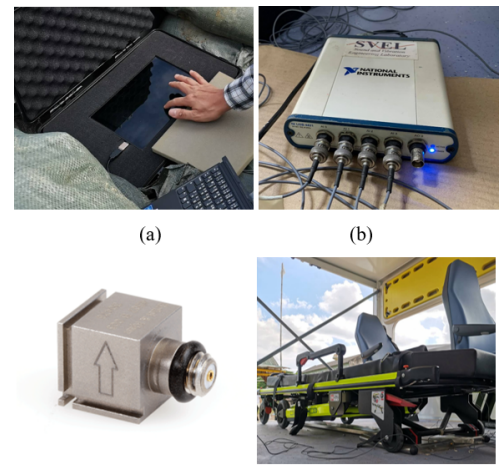

Fig. 13. Shows a device for measuring acceleration and a crash test.

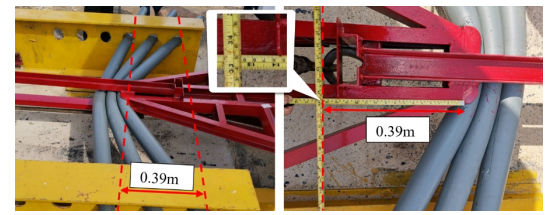

Fig. 14. Shows the deformation of the ladder impact attenuation structure after actual testing.

The acceleration signals were filtered according to SAE-J211 standard by selecting the Channel Filter Class CFC-60 (100 Hz), which measurement signals were smooth and standardized [1, 15, 16, 27, 28]. In this test, the ladder impact attenuation structure of IA5 was selected as the crash testing facility. The sled velocity was measured by radar camera. Fig. 14 shows the deformation of the ladder impact attenuation structure after actual testing, which displacement was 0.39 m and did not exceed the design value.

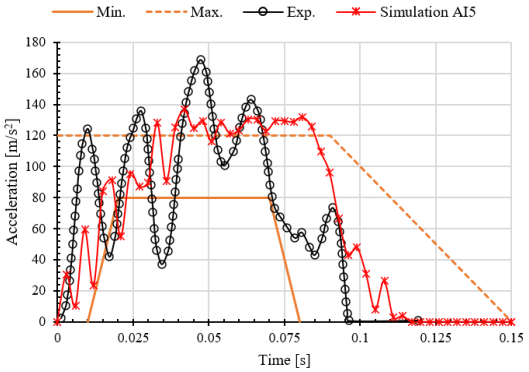

Fig. 15. Validation results.

The simulation result of IA5 was defined with mass 1,386 kg and 9.167 m/s (33 km/h) according to actual testing. Fig. 15 shows the validation results of acceleration profile versus time, the black line-circle for experiment and red line-cross for simulation IA5; it is found that validation was good tendency.

9. Conclusion

This paper presents a use of explicit dynamic simulation to reduce the trial-and-error process in a design of crash test rig that can generate acceleration profile in according to EN1789 standard. The result suggests that this approach is able to give a precise approximation of the acceleration profile up to a certain level.

As a result of this research, a test rig was designed and constructed at a low-cost. The testing capability of the rig is able to test ambulance cabins with mass up to 1,400 kg. This paper also presents a design technique by applying an analytical model and explicit dynamics finite element analysis to specify dimension and geometry of the ladder impact attenuator. The design goal is to create the ladder impact attenuator structure in crash testing facility and to generate acceleration pulse profile accordance to EN1789, which is standard in crashworthiness and crash compatibility for ambulances. The ambulance cabin and medical equipment on the sled crashed at 30-32 km/h and acceleration pulse profile is about 80-120 m/s^2 within 0.9 s and collision end at 0.15 s.

In order to design the impact attenuator structure, the appropriate spring stiffness of the impact attenuator was estimated by using Hooke's Law and a lumped mass system model. The geometry of the impact attenuator structure is placed in a transverse direction as a ladder and has a multi-layered tubular shape to obstruct and absorb crash energy from the sled testing. The crash result was permanent flexural large deformation, but displacement did not exceed 0.5 m. For the reasons mentioned above, the impact attenuation structure was designed to look like a ladder with 2-3 steps.

To ensure that this structure is practical the explicit dynamics finite element model was used to verify and validate with experimental data, which the experimental result and simulation result are consistent tendency. The simulation and test results show that the acceleration profile tends to fit in the suggested acceleration profile as given in EN1789. The experiment showed that the ladder impact attenuator structures can cancel the sled movement within 0.15 s and 0.05 m of displacement. Therefore, the validation result was found that good tendency.

In future studies, we plan to perform crash simulations by explicit dynamics modeling to improve automotive safety and analyze car crashworthiness in order to determine the best structure and materials to use.

Acknowledgements

This research was funded by College of Industrial Technology, King Mongkut's University of Technology North Bangkok (Grant No. Res-CIT0293/2022)

References

[1] Kaya S. Developing test procedure and design of fixture for dynamic test of road ambulances. Middle East Technical University; 2019.

[2] European Committee for Standardization (CEN). Medical vehicles and their equipment - Road ambulances Standard EN 1789:2020. 2020. 1-58 p.

[3] Abramowicz W, Jones N. Dynamic axial crushing of circular tubes. Int J Impact Eng. 1984;2(3): 263-81.

[4] Abramowicz W, Jones N. Dynamic progressive buckling of circular and square tubes. Int J Impact Eng. 1986;4(4): 243-70.

[5] Yadao A, Hingole RS. Modeling and analysis of impact energy absorber by using ls dyna. World J Eng. 2015;12(1): 23-8.

[6] Kusyairi I. The Influence of Origami and Rectangular Crash Box Variations on MPV Bumper with Offset Frontal Test Examination toward Deformability. J Energy, Mech Mater Manuf Eng. 2017;2(2): 89-96.

[7] Kusyairi I, Choiron MA, Irawan YS, Himawan HM. Effects of Origami Pattern Crash Box and Rectangular Pattern Crash Box on The Modelling Of MPV Car Structure on Deformation. J Energy, Mech Mater Manuf Eng. 2018;3(2):61.

[8] Ferdynus M, Kotełko M, Kral J. Energy absorption capability numerical analysis of thin-walled prismatic tubes with corner dents under axial impact. Eksploat i Niezawodn-Maint Reliab. 2018;20(2): 252-89.

[9] Yang C, Li D, Zhu T, Xiao S. Special dynamic behavior of an aluminum alloy and effects on energy absorption in train collisions. Adv Mech Eng. 2016;8(5): 1-9.

[10] Feng Y, Xiao S, Yang B, Zhu T, Yang G, Zhu Z. Dynamic constitutive relation of 5083P-O aluminium alloy and its influence on energy-absorbing structure. Adv Mech Eng. 2018;10(10): 1-13.

[11] J M, A. Keshavarzi. A Numerical and experiment study on the crash behavior of the extruded aluminum crash box with elastic support. Lat Am J Solids Struct. 11: 1329-48.

[12] Santosa S, Wierzbicki T. Crash behavior of box columns filled with aluminum honeycomb or foam. Comput Struct. 1998;68(4): 343-67.

[13] Ghasemnejad H, Hadavinia H, Marchant D, Aboutorabi A. Energy absorption of thin-walled corrugated crash box in axial crushing. SDHM Struct Durab Heal Monit. 2008;4(1): 29-45.

[14] Yang L, Yue M, Li Z, Shen T. An investigation on the energy absorption characteristics of a multi-cell hexagonal tube under axial crushing loads. PLoS One. 2020;15(6).

[15] Segade A, López-Campos JA, Fernández JR, Casarejos E, Vilán JA. Finite element simulation for analysing the design and testing of an energy absorption system. Materials (Basel). 2016;9(8): 1-13.

[16] Vettorello A, Campo GA, Goldoni G, Giacalone M. Numerical-experimental correlation of dynamic test of a honeycomb impact attenuator for a formula sae vehicle. Metals (Basel). 2020;10(5).

[17] Song X, Sun G, Li Q. Sensitivity analysis and reliability based design optimization for high-strength steel tailor welded thin-walled structures under crashworthiness. Thin-Walled Struct [Internet]. 2016;109: 132-42.

[18] Wang D, Zhang S, Wang C, Zhang C. Structure-material-performance integration lightweight optimisation design for frontal bumper system. Int J Crashworthiness. 2018;23(3): 311-27.

[19] Pawlus W, Robbersmyr KG, Karimi HR. Mathematical modeling and parameters estimation of a car crash using data-based regressive model approach. Appl Math Model. 2011;35(10): 5091-107.

[20] Deac SC, Perescu A, Simoiu D, Nyaguly E, Craştiu I, Bereteu L. Modeling and

simulation of cars in frontal collision. IOP Conf Ser Mater Sci Eng. 2018;294(1).

[21] Gokhale NS, Deshpande SS, Bedekar S V, Thite AN. Book-Nitin S gokhale ,sanjay S deshpande-practical finite element analysis.pdf. 2008. p. 445.

[22] Yadav S, Pradhan SK. Investigations into dynamic response of automobile components during crash simulation. Procedia Eng [Internet]. 2014;97: 1254-64.

[23] Liu Y. ANSYS and LS-DYNA used for structural analysis. Int J Comput Aided Eng Technol. 2008;1(1): 31-44.

[24] Villavicencio R, Sutherland L, Guedes Soares C. Numerical simulation of transversely impacted, clamped circular aluminium plates. Ships Offshore Struct. 2012;7(1): 31-45.

[25] Jia LJ. Integration algorithm for a modified Yoshida-Uemori model to simulate cyclic plasticity in extremely large plastic strain ranges up to fracture. Comput Struct [Internet].2014;145: 36-46.

[26] Livermore Software Technology Corp. LS-Dyna Theory Manual. Vol. 19. Livermore, California; 2019.

[27] Grenke BD. Digital filtering for J211 requirements using a fast fourier transform based filter. SAE Tech Pap. 2002;(724).

[28] Society of Automotive Engineers. Instrumentation for Impact Test-Part 1-Electronic Instrumentation J211/1_201403. Soc Automot Eng. 2014;552(724): 1-12.